

# Chronic Pelvic Pain Development and Prostate Inflammation in Strains of Mice With Different Susceptibility to Experimental Autoimmune Prostatitis

Maria L. Breser, Ruben D. Motrich, Leonardo R. Sanchez, and Virginia E. Rivero\*

*Centro de Investigaciones en Bioquímica Clínica e Inmunología (CIBICI-CONICET), Departamento de Bioquímica Clínica, Facultad de Ciencias Químicas, Universidad Nacional de Córdoba, Haya de la Torre y Medina Allende, Ciudad Universitaria, Córdoba, Argentina*

**BACKGROUND.** Experimental autoimmune prostatitis (EAP) is an autoimmune inflammatory disease of the prostate characterized by peripheral prostate-specific autoimmune responses associated with prostate inflammation. EAP is induced in rodents upon immunization with prostate antigens (PAg) plus adjuvants and shares important clinical and immunological features with the human disease chronic prostatitis/chronic pelvic pain syndrome (CP/CPPS).

**METHODS.** EAP was induced in young NOD, C57BL/6, and BALB/c male mice by immunization with PAg plus complete Freund's adjuvant. Tactile allodynia was assessed using Von Frey fibers as a measure of pelvic pain at baseline and at different time points after immunization. Using conventional histology, immunohistochemistry, FACS analysis, and protein arrays, an interstrain comparative study of prostate cell infiltration and inflammation was performed.

**RESULTS.** Chronic pelvic pain development was similar between immunized NOD and C57BL/6 mice, although the severity of leukocyte infiltration was greater in the first case. Conversely, minimal prostate cell infiltration was observed in immunized BALB/c mice, who showed no pelvic pain development. Increased numbers of mast cells, mostly degranulated, were detected in prostate samples from NOD and C57BL/6 mice, while lower total counts and resting were observed in BALB/c mice. Prostate tissue from NOD mice revealed markedly increased expression levels of inflammatory cytokines, chemokines, adhesion molecules, vascular endothelial growth factor, and metalloproteinases. Similar results, but to a lesser extent, were observed when analyzing prostate tissue from C57BL/6 mice. On the contrary, the expression of the above mediators was very low in prostate tissue from immunized BALB/c mice, showing significantly slight increments only for CXCL1 and IL4.

**CONCLUSIONS.** Our results provide new evidence indicating that NOD, C57BL/6, and BALB/c mice develop different degrees of chronic pelvic pain, type, and amount of prostate cell infiltration and secretion of inflammatory mediators. Our results corroborate and support the notion that mice with different genetic background have different susceptibility to EAP induction. *Prostate* © 2016 Wiley Periodicals, Inc.

**KEY WORDS:** pelvic pain; prostate; inflammation; mast cells; CPPS; prostatitis

---

Grant sponsor: Agencia Nacional de Promoción Científica y Tecnológica (ANPCyT) PICT; Grant numbers: 2008-1639; 2013-2201; Grant sponsor: Secretaría de Ciencia y Técnica de la Universidad Nacional de Córdoba (SECyT-UNC).

Conflicts of interest: No potential conflicts of interest were disclosed.

\*Correspondence to: Dr. Virginia Rivero, Centro de Investigaciones en Bioquímica Clínica e Inmunología (CIBICI-CONICET), Departamento de Bioquímica Clínica, Facultad de Ciencias Químicas, Universidad Nacional de Córdoba, Haya de la Torre y Medina Allende, Ciudad Universitaria, 5016 Córdoba, Argentina. E-mail: vrivero@fcq.unc.edu.ar

Received 25 June 2016; Accepted 28 August 2016

DOI 10.1002/pros.23252

Published online in Wiley Online Library  
(wileyonlinelibrary.com).

## INTRODUCTION

Chronic prostatitis/chronic pelvic pain syndrome (CP/CPSP), or category III prostatitis, accounts for more than 90% of all cases of prostatitis, affecting 10–14% of men of all ethnic origins and being the most common urologic morbidity in men younger than 50 years old [1,2]. CP/CPSP is characterized by chronic pelvic pain and signs and symptoms of prostate inflammation in the absence of infection [3,4]. Its etiology is still unknown and effective treatments are limited. A significant advance in the understanding of CP/CPSP was made when an autoimmune Th1 response against prostate antigens was revealed in a considerable number of patients, proposing an autoimmune basis for CP/CPSP [5,6].

Extensive work has been done regarding the development and characterization of rodent models of experimental autoimmune prostatitis (EAP) that could be considered as appropriate animal models for CPSP [7,8]. The immunization with a mixture of PAg plus adjuvants in young male NOD mice induces peripheral autoreactive pathogenic T cells, autoantibody responses as well as inflammation and infiltration in the prostate [9,10]. This model showed almost all the characteristics of human chronic autoimmune prostatitis: specific lymphocytes against prostate antigens, the secretion of IFN $\gamma$  in lymphocytes culture supernatants and the infiltration and histological lesions typically observed in prostate tissue [5,7,11].

The genetic background and hormonal imbalances are factors that could contribute to the onset of the disease in susceptible young males [12,13]. Studies focused on differential susceptibility to the development of EAP have shown that NOD, C57BL/6, SJL, AJ, and BALB/c mice exhibited different degrees of severity of prostatic inflammation after EAP induction, being NOD, and BALB/c mice the most susceptible and the most resistant strains, respectively [7,14]. NOD mice develop severe prostate inflammation, accompanied by specific T cell-mediated responses that could be assessed by *in vitro*-specific proliferation and IFN $\gamma$  secretion [9,15,16]. A crucial role of IFN $\gamma$  in EAP has been shown because the absence of IFN $\gamma$  or transcription factors involved in the IFN $\gamma$  signaling cascade, made mice resistant to EAP induction [15,16]. Also, the expression of the Th1-associated chemokine receptors CXCR3 and CCR5 on prostate-specific effector T cells was shown to be associated with their homing and infiltration of the prostate [17].

As mentioned, EAP is differentially induced in NOD and C57BL/6 but not in BALB/c mice [14,17]. While numerous disease characteristics have already been described, the comparative analysis among strains of experienced pelvic pain, the presence and

amount of different inflammatory mediators and degree of prostate leukocyte infiltration remain to be explored.

In the present work, we conducted a comparative analysis of these aspects in NOD, C57BL/6, and BALB/c mice. Our results show that pelvic pain development was comparable between NOD and C57BL/6 mice, although the amount of leukocyte infiltration was greater in the first case. Noteworthy, comparable high numbers of degranulated mast cells were observed in prostate tissue from these mice. Also, NOD mice showed strongly increased expression levels of different inflammatory mediators in prostate tissue, followed by C57BL/6 mice who expressed intermediate-to-mild levels. On the other hand, BALB/c mice did not develop chronic pelvic pain. In agreement, prostate leukocyte infiltration was minimal and with variable cell composition in these mice. Moreover, low levels of resting mast cells were observed. Finally, BALB/c mice only showed a slight increase in some of the inflammatory mediators assayed.

## MATERIALS AND METHODS

### Mice and Antigens

Mouse strains used in this study were NOD/LtJ (NOD/ShiLtJ), C57BL/6 and BALB/c purchased from The Jackson Laboratory (Bar Harbor, ME). All animals were housed and maintained under SPF conditions in the Animal Facilities of the Facultad de Ciencias Químicas, Universidad Nacional de Córdoba and used at the age of 6–8 weeks. All animal experiments were approved by and conducted in accordance with guidelines of the Committee for Animal Care and Use of the Facultad de Ciencias Químicas, Universidad Nacional de Córdoba, and the ethics committee of the Institute CIBICI (Protocol number 954/2016), in strict accordance with the recommendation of the Guide to the Care and Use of Experimental Animals published by the Canadian Council on Animal Care (OLAW Assurance number A5802-01) and the Portuguese State Veterinary Division (DGV).

The preparation of a mixture of PAg and the purification of Prostatein or prostate steroid-binding protein (PSBP) were performed as previously described (18). The purity of the PSBP preparation was >95% as evaluated by Western blot and was LPS-free as tested by Gel clot 0.03 endotoxin units/ml sensitivity (Charles River, Laboratories International, Wilmington, NY).

### Antibodies

Commercially available antibodies used in different experiments performed and their respective

manufacturers were as follows: anti-CD4 (RM4-5), anti-CD11b (M1/70), anti-CD3 (145-2C11), anti-GR1 (RB6-8C5); and IgG isotype controls were purchased from BD Biosciences (San Diego, CA). Anti-CD45 (30-F11) Anti-CD8a (53-6.7) was purchased from eBioscience (San Diego, CA). Anti-CD45 (30-F11) and anti-CD11b (M1/70) were purchased from BioLegend.

### EAP Induction and Prostatitis Histological Score

Six- to 8-week-old male NOD, C57BL/6 and BALB/c mice were subcutaneously immunized in the hind footpad and in the base of the tail with PAg (300 µg/mouse) or saline solution emulsified in CFA (Sigma-Aldrich, St. Louis, MO) in a total volume of 150 µl/mouse. Mice received immunizations at days 0 and 15, and then were sacrificed at day 24 of the experimental schedule [17,18]. As previously described [18], the severity of EAP was assessed by determining the histological score, which was analyzed in a double-blind manner and computed for individual glands by summing the pathologic grade of each prostate tissue section and dividing it by the total number of sections examined. The degree of inflammation was assessed using a score of 0–3: 0, no inflammation; 1, mild but definite perivascular cuffing with mononuclear cells; 2, moderate perivascular cuffing with mononuclear cells; 3, marked perivascular cuffing, hemorrhage, and numerous mononuclear cells in the parenchyma, in 5-mm-thick prostate tissue sections of each organ per animal that were processed by conventional hematoxylin and eosin staining. For the identification of mast cells prostate tissue sections were stained in 0.02% toluidine blue for 5 min. Mast cell were considered degranulated/activated if (at 400× magnification) extracellular granules, indistinct boundaries, uneven staining of various parts of the cell, or distinct intracellular vacuolization within the cells were observed. Mast cells, degranulated/activated and resting, were counted in a blinded manner in non-serial quadruplicate tissue sections. Slides were visualized in a microscope Nikon TE 2000U (Nikon, Osaka, Japan), and pictures were analyzed using the Adobe Photoshop CS6 version 13 image analysis software (Adobe Systems, Inc., San Jose, CA).

### Immunohistochemistry Assays

Formalin-fixed and paraffin-embedded prostate tissue sections were dewaxed in xylene, rehydrated, treated with Target Retrieval Solution (DakoCytomation, Glostrup, Denmark) at 95°C for 30 min, and blocked with Fc blocking solution (BD Bioscience). Endogenous peroxidase activity was blocked with blocking buffer (DakoCytomation). Then slides were

incubated overnight at 4°C in blocking buffer containing rabbit anti-CD45 (clone 30-F11) Abs. Slides were washed four times in 10 mM PBS, 0.1% Tween 20, and incubated with anti-rabbit HRP (BD Bioscience) secondary Abs for 2 hr at room temperature. Colorimetric detection was performed by using Detection Kit (BD Bioscience) and counterstained with hematoxylin.

### Analysis of Prostate-Infiltrating Leukocytes

Prostate-infiltrating leukocyte analysis was performed as previously described [17,19]. Freshly harvested prostate tissue samples were mechanically disrupted and enzymatically digested in RPMI 1640-GlutaMAX medium (Life Technologies, Carlsbad, CA) medium containing 1 mg/ml collagenase D (Roche, Basel, Switzerland) and DNase I (Sigma-Aldrich) for 45 min at 37°C. After digestion, suspensions were filtered through 75-mm and 40-mm cell strainers (BD Biosciences), and single cell suspensions were washed twice in 10% fetal bovine serum (Life Technologies), 2 mM EDTA, and 50 mM 2-mercaptoethanol supplemented RPMI 1640 medium. Live lymphocyte counts were deduced from the acquisition of a fixed number of 10 mm latex beads (Beckman Coulter, Brea, CA) mixed with a known volume of unstained cell suspension in propidium iodide (BD Biosciences). Analyses were performed on a FACSCanto II using DIVA software (BD Biosciences), allowing the exclusion of dead cells (propidium iodide positive) inside the indicated gates. After that, cells were stained with different antibodies for flow cytometry analysis. Cells were acquired using a FACSCanto II, and data were analyzed using FlowJo software (Tree Star Inc., Ashland, OR).

### Chronic Pelvic Pain Assessment by Behavioral Testing

Chronic pelvic pain development was assessed by behavioral testing, as previously described [19,20]. Behavior testing was based on the concept of cutaneous hyperalgesia resulting from referred visceral pain [21]. An irritable focus in visceral tissues reduces cutaneous pain thresholds, allowing for an exaggerated response to normally non-painful stimuli (allodynia). Mice under study were tested for allodynia before immunization (baseline, day 0) and at 7, 14, and 24 days post immunization (dpi). As previously described (19), tests were performed in individual acrylic glass chambers with a stainless steel wire grid floor (mouse acclimation period of 20 min before testing). Referred hyperalgesia and tactile allodynia were tested using von Frey filaments with forces of 0.04, 0.16, 0.4, 1, and 4 g (Bioseb, Chaville, France).

Each filament was applied for 1–2 sec with an inter-stimulus interval of 5 sec for a total 10 times, and the filaments were tested in ascending order of force. Stimulation was confined to the lower abdominal area in the general vicinity of the prostate, and care was taken to stimulate different areas within this region to avoid desensitization or “windup” effects. An investigator blinded to the treated group graded responses in animals. Three types of behaviors were graded as positive responses to filament stimulation: (i) sharp retraction of the abdomen; (ii) immediate licking or scratching of the area of filament stimulation; or (iii) jumping. Response frequency was calculated as the percentage of positive response, and data were reported as the mean percentage of response frequency  $\pm$  SEM.

### Analysis of Inflammation Markers Expression in Prostate Tissue

Prostates from control and immunized animals were obtained and excised at day 24 of the experimental schedule, and the expression levels of a panel of 96 cytokines, chemokines and other inflammatory molecules in tissue samples were measured using a mouse cytokine/chemokine array kit (Ray Biotech, Norcross, GA) following manufacturer’s instructions and software.

### Statistics

Statistical analysis was performed using one-way or two-way ANOVA with Bonferroni post hoc test analysis. Mean  $\pm$  SEM are represented in the graphs. Statistical tests were performed using the GraphPad Prism 5.0 software. The *P* values ( $*P < 0.05$ ,  $**P < 0.01$ ,  $***P < 0.001$ ) were considered significant in all analyses. Given the number of observations, sample means, and SD, a compromise power analyses using G\*Power3 data analysis software was performed to determine the statistical power ( $>0.96$ ) to exclude the possibility of type II error.

## RESULTS

### Pelvic Pain Development and Prostate Cell Infiltration After EAP Induction

To assess if chronic pelvic pain development was detectable in the strains of mice under study, NOD, C57BL/6 and BALB/c mice were tested for suprapubic allodynia at baseline and over time after PAg immunization. Mechanical stimulation of the pelvic area of PAg-immunized mice resulted in a response frequency that correlated with the applied force [22],

and this response profile was similar for NOD and C57BL/6 mice (Fig. 1). Significant increases were detected at 14 and 24 dpi in immunized NOD mice showing pelvic pain development (Fig. 1A). Similar results were observed in immunized C57BL/6 mice, showing significant increases in tactile allodynia at earlier time points (Fig. 1B). However, no increases in tactile allodynia responses over time were observed in immunized BALB/c mice (Fig. 1C).

To assess if the development of pelvic pain was accompanied by prostate tissue inflammation and leukocyte infiltration, conventional histology and immunohistochemistry assays were performed on prostate tissue sections from animals under study (Fig. 2). Significant histological alterations were detected in all anatomical regions of the prostate gland (ventral, dorsal, and coagulating gland) from immunized NOD mice. These alterations consisted in multifocal perivascular and stromal mononuclear cell infiltration accompanied by edema and severe tissue disorganization, being the EAP histopathological score for this strain  $2.86 \pm 0.22$  (Fig. 2A and B). Prostate tissue sections from immunized C57BL/6 mice also exhibited focal perivascular and stromal mononuclear cell infiltration accompanied by edema, and showing an EAP score of  $1.9 \pm 0.26$  (Fig. 2A and B). Conversely, prostate tissue sections from immunized BALB/c mice showed no significant histological changes with an EAP score of  $0.20 \pm 0.10$  (Fig. 2A and B). Immunohistochemistry assays revealed a marked CD45<sup>+</sup> cell infiltration in different parts of the prostate gland of immunized NOD mice (Fig. 2C). Focal aggregates of CD45<sup>+</sup> cell were detected in the case of immunized C57BL/6 prostate tissue sections, whereas almost no CD45<sup>+</sup> infiltration could be observed in prostate sections from immunized BALB/c mice (Fig. 2C). In addition, the presence of mast cells was identified by toluidine blue staining. Significantly increased numbers of mast cells, most of them in an activated/degranulated state, were observed in prostate tissue from immunized NOD and C57BL/6 mice (Fig. 2D and E). In contrast, lower mast cell counts with the majority of them in a resting state were observed in prostate tissue from immunized BALB/c mice (Fig. 2D and E).

These results show that pelvic pain development after PAg immunization is strain specific and is accompanied by inflammation, mononuclear and mast cell infiltration in the prostate.

### Analysis of Prostate Infiltrating Leukocytes After EAP Induction

We next quantified and characterized prostate infiltrating leukocytes by performing FACS analysis (Fig. 3).

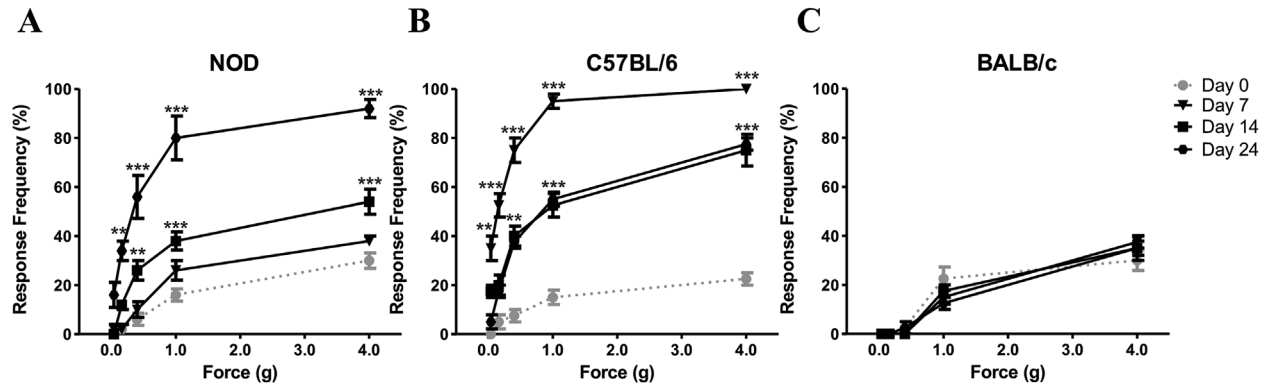


**Fig. 1.** Chronic pelvic pain development in NOD, C57BL/6, and BALB/c mice after PAg immunization. Young male NOD, C57BL/6, and BALB/c mice were immunized with PAg emulsified in CFA and referred visceral hyperalgesia was measured over time of EAP induction as responses to mechanical stimulation of the pelvic region and hind paw using von Frey filaments of 5 calibrated forces. Data are shown as the mean percentage of response frequency  $\pm$  SEM (e.g., 5 responses of 10 = 50%) before (baseline, day 0) or at 7, 14, and 24 days post immunization (dpi). **(A)** Tactile allodynia responses to pelvic stimulation of immunized NOD **(A)**, C57BL/6 **(B)**, and BALB/c **(C)** mice over different time points after EAP induction. Data are shown as mean  $\pm$  SEM,  $n=5$  per group, and are representative of 3 independent experiments with essentially the same results. The  $P$  values were obtained using one-way ANOVA followed by Bonferroni post hoc test analysis. \* $P < 0.05$ .

In remarkable concordance with the histopathological scores, the amounts of leukocytes ( $CD45^+$ ) recovered from prostate tissues from immunized NOD mice were higher than those from immunized C57BL/6 animals (about threefold). On the other hand, immunized BALB/c presented mild to absent prostate leukocyte infiltration (Fig. 3A and B). Remarkably, about 35% of the prostate infiltrating leukocytes in immunized NOD and C57BL/6 mice shown to be  $CD3^+$ T lymphocytes, with higher proportions of  $CD4^+$  than  $CD8^+$  cells. Also,  $CD11b^+$  and  $GR1^+$  cells were other important populations present in prostate tissue infiltrates, while  $CD19^+$ B lymphocytes were found in low proportions (Fig. 3C). Regarding prostate tissue infiltration in immunized BALB/c mice, low quantities of  $CD45^+$  cells were found. In addition, immunized BALB/c mice also showed a different cellular composition when compared to immunized NOD and C57BL/6 mice, with minor proportions of  $CD3^+$ T lymphocytes and higher frequencies of  $GR1^+$  granulocytes. These results show that although C57BL/6 mice exhibit fewer prostate cell infiltrates than NOD mice, the composition was very similar in both strains. On the other hand, BALB/c mice not only showed 20 times less tissue cell infiltration but also infiltrates with a different cell composition.

#### Inflammatory Markers Expression in Prostate Tissue After EAP Induction

We next analyzed the expression of different cytokines, chemokines, and inflammatory mediators in prostate tissue homogenates from immunized mice under study using a protein super array. Prostate

tissue from immunized NOD mice showed higher expression levels of  $IFN\gamma$ , IL-17A, IL-12p40, and IL-12p70, whereas lower values were detected in prostate tissue from immunized C57BL/6 mice. On the contrary, very low levels of these inflammatory cytokines were detected in prostate tissue from immunized BALB/c mice (Fig. 4A and B). No differences in IL-10 expression levels were found among the mice strains under analysis. However, prostate tissue from immunized BALB/c mice showed increased expression levels of IL-4. Regarding IL-1 $\alpha$ , IL-1 $\beta$ , IL-6, TNF $\alpha$ , and CXCL1, elevated levels were detected in prostate tissue from immunized NOD mice, followed by lower values in immunized C57BL/6 mice and much lower amounts in immunized BALB/c mice.

A similar expression pattern among mice strains under study was observed for chemokines CXCL9, CXCL10, CXCL11, CCL3, CCL4, CCL5, CCL2, CCL22, CCL9, and CCL20. The highest values were found in prostate tissue from immunized NOD mice, moderate levels in prostate tissue from immunized C57BL/6 mice and very low levels in prostate tissue from immunized BALB/c mice (Fig. 5A–C). Regarding adhesion molecules, prostate tissue samples from immunized NOD mice once again exhibited the major levels of expression followed by immunized C57BL/6 and BALB/c mice, respectively (Fig. 5D). The same pattern was observed for VEGF and VEGF-D expression, which showed the highest expression levels in prostate tissue from immunized NOD mice (Fig. 5E).

Finally, we also evaluated the expression of metalloproteinases (MMPs). Significantly increased values of MMP2 expression were detected in prostate tissue

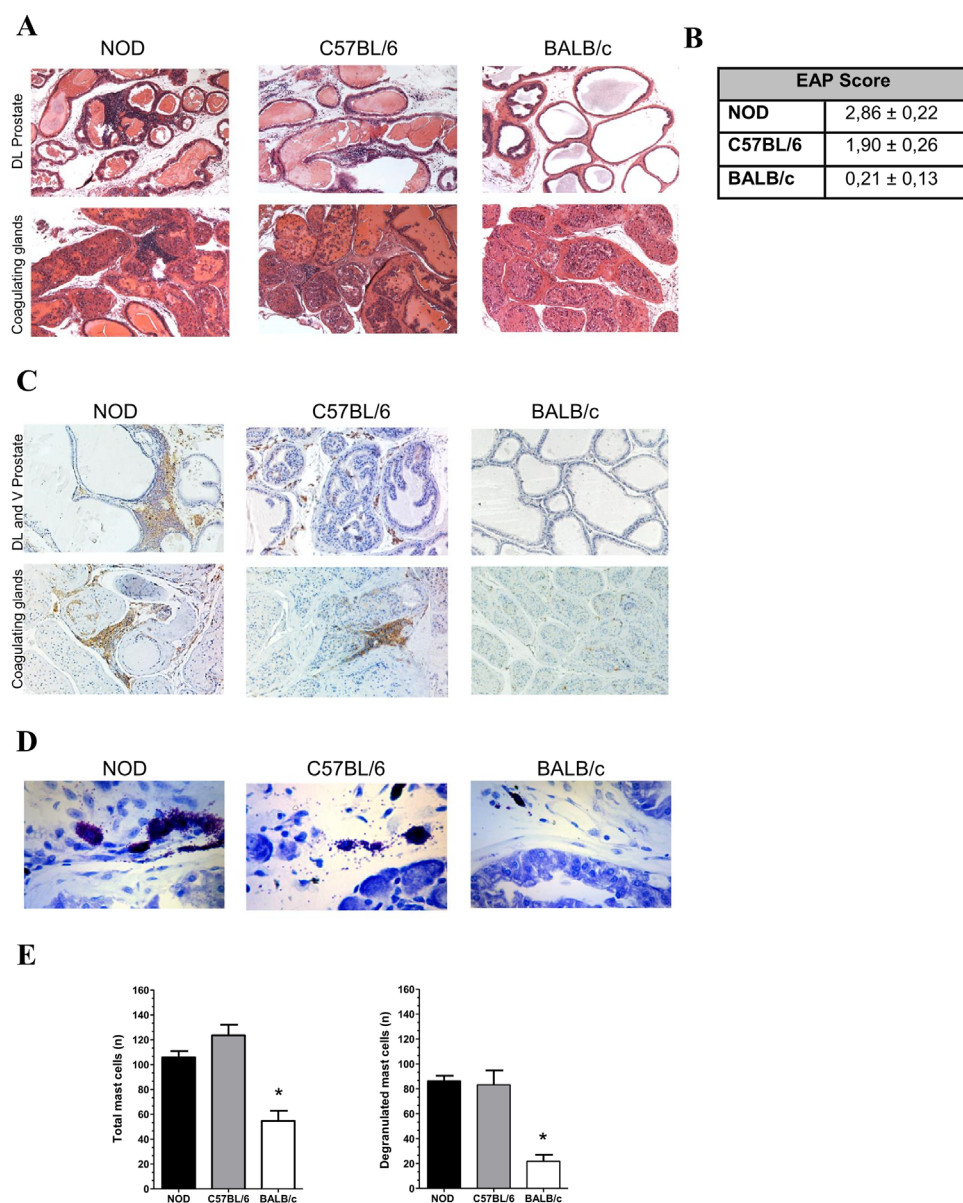


**Fig. 2.** Histological alterations and cell infiltration in prostate tissue from NOD, C57BL/6, and BALB/c mice after EAP induction. NOD, C57BL/6, and BALB/c mice were treated as in Figure 1. On day 24, mice were euthanized and the prostate glands excised. **(A)** Prostate histopathology scores and representative hematoxylin-eosin staining assays performed in prostate tissue sections from immunized NOD, C57BL/6, and BALB/c mice. Original magnification: 200 $\times$ . **(B)** EAP score from mice under study. **(C)** Representative immunohistochemistry assays for the detection of CD45<sup>+</sup> cells in prostate tissue from immunized NOD, C57BL/6, and BALB/c mice analyzed at 24 dpi. **(D)** Mast cell in toluidine blue stained prostate tissue sections from PAG immunized NOD, C57BL/6, and BALB/c mice. Total and activated/degranulated mast cell numbers were determined in a blinded manner in non-serial sections of prostate tissue stained with toluidine blue. Mast cell counts are expressed as number of cells/tissue section analyzed. Data are shown as mean  $\pm$  SEM; n = 5 per group and are representative of 3 independent experiments with essentially the same results. The *P* values were obtained using one-way ANOVA followed by Bonferroni post hoc analysis.

from immunized NOD and C57BL/6 mice, while the expression of MMP3 was increased in prostate tissue from immunized BALB/c mice (Fig. 5F).

Altogether, these results indicate that, after immunization, NOD mice show strongly increased expression of inflammatory cytokines, chemokines, adhesion molecules, vascular endothelial growth factor, and

metalloproteinases. In the case of C57BL/6 mice, moderate to high increases of all these inflammatory mediators were also detected in prostate tissue after PAG immunization. However, in immunized BALB/c mice, the expression of those mediators was very low, only showing increments in the expression of IL-4, CXCL1, and MMP3.

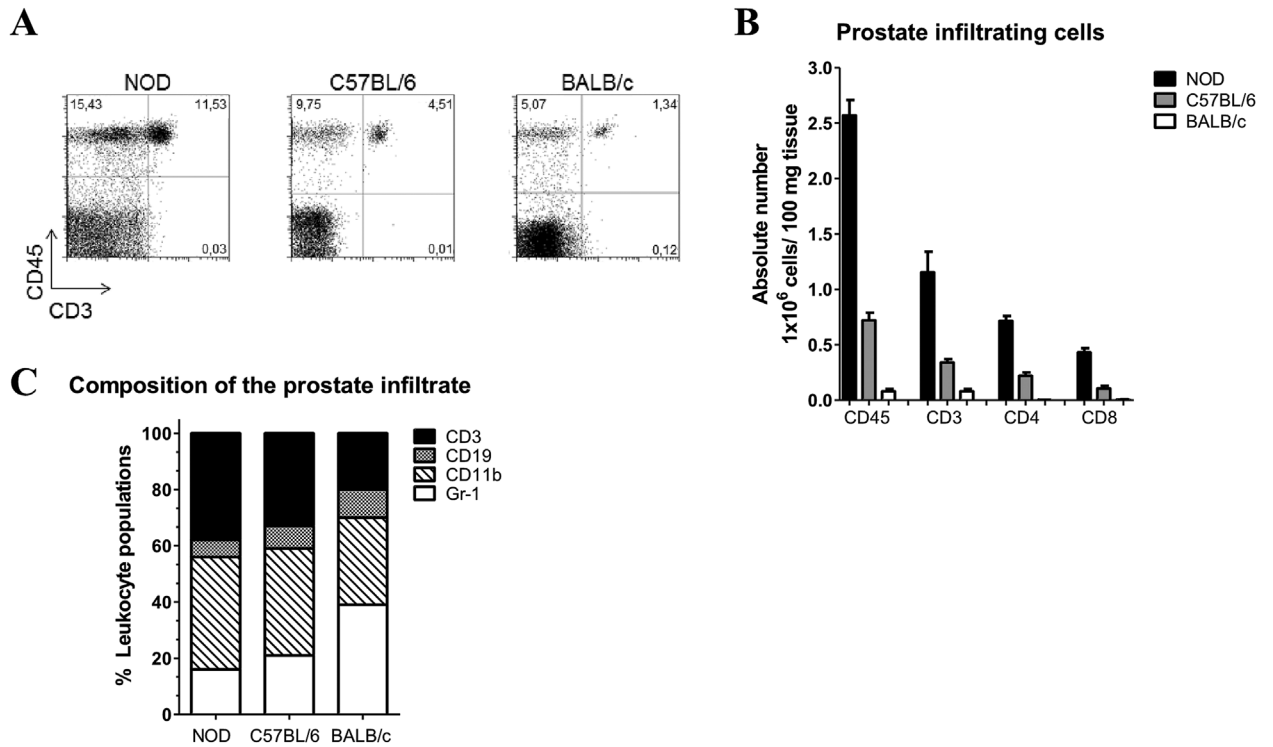


**Fig. 3.** Prostate tissue cell infiltration in NOD, C57BL/6, and BALB/c mice after EAP induction. Mice under study were euthanized and the prostates were excised at day 24 after PAg immunization and processed for flow cytometry analysis. Live cells were counted, and flow cytometry was performed to evaluate leukocyte infiltration in the glands. **(A)** Representative flow cytometry dot plots of the analysis of different leukocyte subpopulations: CD45<sup>+</sup> versus CD3<sup>+</sup> cells. Numbers indicate the percentage of cells in each quadrant. **(B)** Absolute number of CD45<sup>+</sup>, CD3<sup>+</sup>, CD4<sup>+</sup> and CD8<sup>+</sup> cells in the prostate gland from mice under study. **(C)** Composition of the prostate infiltrates in NOD, C57BL/6 and BALB/c mice. Data are shown as mean ± SEM; n = 5 per group and are representative of 3 independent experiments with essentially the same results.

**DISCUSSION**

As EAP has been proposed as a reliable animal model for the study of the human disease CPPS [7,8],

we here analyzed the induction of autoimmune prostatitis and chronic pelvic pain development upon PAg immunization in three different strains of mice commonly used in basic research. We comparatively

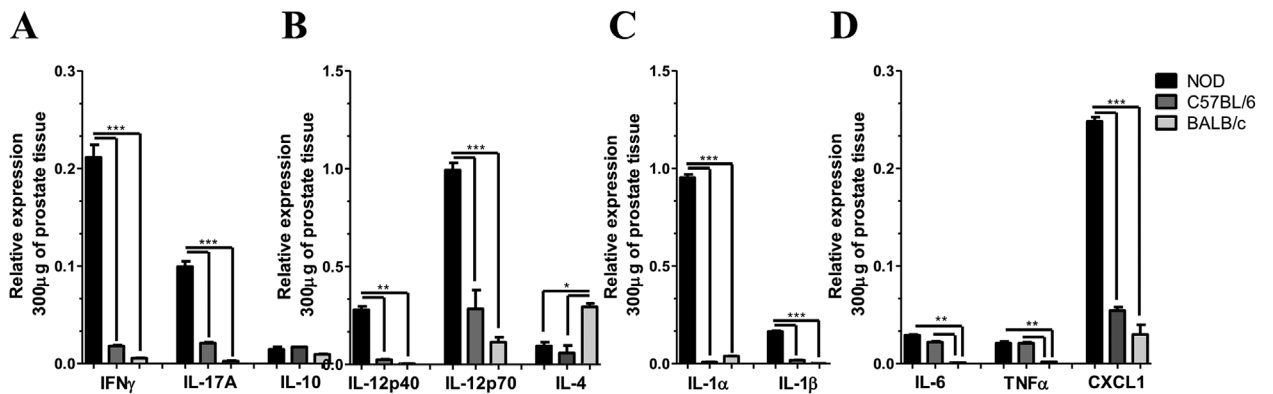


**Fig. 4.** Relative protein expression of cytokines in prostate tissue from immunized NOD, C57BL/6, and BALB/c mice. Prostates from PAg immunized animals were obtained and excised at day 24 after immunization, and protein levels of different cytokines in tissue samples were measured. **(A)** IFN $\gamma$ , IL-17A, and IL-10. **(B)** IL-12p40, IL-12p70, and IL-4. **(C)** IL-1 $\alpha$  and IL-1 $\beta$ . **(D)** IL-6, TNF $\alpha$ , and CXCL1. Data are shown as mean ± SEM, n = 5 per group, and are representative of two independent experiments. The P values were obtained using one-way ANOVA followed by Bonferroni post hoc analysis.

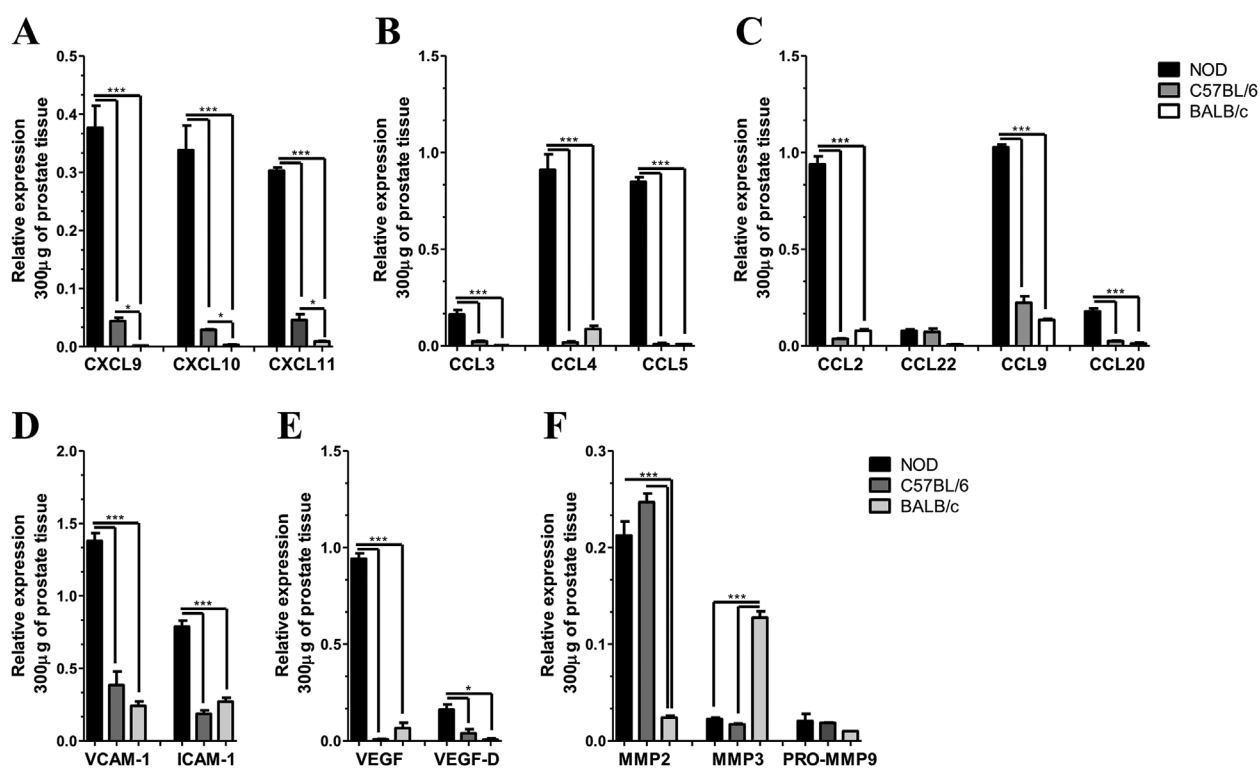


**Fig. 5.** Relative protein expression of chemokines and other inflammatory mediators in prostate tissue from immunized NOD, C57BL/6, and BALB/c mice. Prostates from PAg immunized animals were obtained and excised at day 24 after immunization, and chemokines levels in tissue samples were measured. **(A)** CXCL9, CXCL10, and CXCL11. **(B)** CCL3, CCL4, and CCL5. **(C)** CCL2, CCL22, CCL9, and CCL20. **(D)** VCAM-1 and ICAM-1. **(E)** VEGF and VEGF-D. **(F)** MMP2, MMP3, and PRO-MMP9. Data are shown as mean  $\pm$  SEM,  $n = 5$  per group, and are representative of two independent experiments. The  $P$  values were obtained using one-way ANOVA followed by Bonferroni post hoc analysis.

analyzed different parameters such as chronic pelvic pain, histological damage, type and amount of leukocyte infiltration and the expression of various inflammatory mediators in prostate tissue. Our results corroborate that mice with different genetic background have different susceptibility to EAP induction, showing differences in all the assayed clinical and pathological parameters: chronic pelvic pain, type and amount of tissue cell infiltration and inflammatory mediator levels.

Susceptibility to autoimmune diseases results from the encounter of a complex and long evolved genetic context with a no less complex and changing environment. It could be assumed that the three strains of mice under study have differences in MHC-antigen complexes number or affinity [23] and different selection of TCR repertoire resulting in the purging of autoreactivity, being this process more or less efficient in every strain [24]. However, in most models of immunization with self-protein, antigen specific immune response can be detected irrespective whether disease follows or not, indicating that other layers of immune control, beyond the engagement of effector cells, condition the evolution to disease [25].

In the case of EAP, disease is clearly evidenced by the infiltration and damage in the prostate gland [9,10]. Similar to that observed in CP/CPSP, the development of chronic pelvic pain during EAP induction has recently been demonstrated [19,20]. It has been shown that chronic pelvic pain developed in parallel with prostate tissue leukocyte infiltration [19,26]. Interestingly, results from the present work indicate that tactile allodynia responses in NOD and C57BL/6 mice show comparable values, although NOD mice exhibit approximately three times more leukocyte infiltration and higher expression of inflammatory mediators in the target organ. In addition, C57BL/6 mice exhibit fewer tissue cell infiltrates than NOD mice but the cellular composition was very similar in both strains. Conversely, BALB/c mice exhibit no allodynia responses over time although they develop peripheral prostate specific immune response upon immunization [17]. It was recently been shown that prostate-specific T cells induced upon PAg immunization express CXCR3 and CCR5 chemokine receptors and migrate to and infiltrate the prostate gland [19]. Once there, these lymphocytes induce the local secretion of several cytokines and



chemokines, which in turn recruit more leukocytes augmenting tissue cell infiltration and enhancing prostate inflammation [27,28]. Whether chronic pelvic development is directly linked to tissue T cell infiltration, C57BL/6 mice should exhibit lower allodynia responses.

The development of chronic pelvic pain could be associated with a particular mediator or cell type present in the infiltrates [29,30]. Mast cells are currently suggested as the main mediators and effector cells in disease progression from initiation to breaking of tolerance, neuronal activation, and, eventually, sensitization [30,31]. Mast cells contribute to rapidly occurring neuronal peripheral sensitization, which is mediated by nerve growth factor (NGF) [32]. They are known to express TrkA receptors on their cell membrane [26]. In addition, it has been reported that macrophages and NK cells also express TrkA receptors [33,34]. It is possible that binding of NGF to TrkA receptors on mast cells might cause degranulation, establishing a feedback mechanism that would promote sensitization [26]. In the present report, we provide evidence showing that comparable increased mast cell counts, and also in an activated state, were present in prostate tissue from immunized NOD and C57BL/6 mice, strains that developed similarly increased tactile allodynia responses. It has been shown that CP/CPPS patients have elevated levels of mast cell tryptase-b, carboxypeptidase A3, and NGF in expressed prostate secretions and urine. Moreover, NGF levels directly correlated with pain severity [35,36]. These results suggest that NGF and mast cells secretion products are potential mediators involved in peripheral pain sensitization mechanisms in CP/CPPS. The presence of markedly increased numbers of mast cells in prostate cell infiltrates in EAP was already reported by us and other groups [37,38]. Noteworthy, most mast cells evidenced an activated state because a high proportion of them shown to be degranulated and secreted pain inducer molecules, such as tryptase-b and NGF [37,38].

In the present work, elevated levels of several chemokines were also detected in prostate tissue from immunized NOD mice. Many of these chemotactic factors, as CXCL9, CXCL10, CXCL11, and CCL20, have been reported to be involved in the recruitment of Th1 and Th17 cells [39,40,41]. In concordance with these increased levels of chemokines, higher proportions of CD3<sup>+</sup> cells were detected in prostate tissue from NOD mice. Regarding BALB/c mice, the minimum prostate cell infiltration observed showed a different leukocyte composition. In fact, GR1<sup>+</sup> cell were predominant in tissue cell infiltrates in BALB/c mice in concordance with the increment of CXCL1, the only chemokine that was found increased in the prostate from these mice.

Indeed, CXCL1 has been associated with the recruitment of GR1<sup>+</sup> cells to other tissues [42].

The endothelial adhesion molecules ICAM-1 and VCAM-1 are known as central mediators of leukocyte adhesion to and transmigration across the endothelium [43]. In addition to augmented leukocyte infiltration in prostate tissue, increased adhesion molecules and vascular endothelial factors levels were observed in prostate tissue from NOD mice and also, but to a certain extent, in C57BL/6 mice. Using a murine model of chronic non-bacterial prostatitis that develops spontaneously with age, Wilson et al. [44] showed that MMPs have a role in the pathogenesis of the disease, which may involve destruction of extracellular matrix proteins. These MMPs can also induce the release of growth factors, especially angiogenic factors, thus affecting the microenvironment [44,45]. In the present work, enhanced expression of MMP-2 was detected in prostate tissue from NOD and C57BL/6 mice, while increased MMP-3 levels were found in prostate tissue from BALB/c mice. A fundamental aspect of inflammation is the infiltration of interstitial tissue by leukocytes, which in turn secrete several potent proteinases such as MMPs that facilitate the clearance of foreign agents and remove damaged cells and extracellular matrix [46]. It has been reported that macrophages infiltrating the prostate can secrete MMP-1, -2, -3, -7, -9, and -12; neutrophils secrete MMP-9 and -8; and lower levels of MMP-2 and -9 are produced by lymphocytes [47,48]. In the present work, the observed increased levels of MMP-2 and -3 could be attributed to macrophages and lymphocytes infiltrating the prostate gland.

In conclusion, our results provide new evidence indicating that NOD, C57BL/6, and BALB/c mice develop different degrees of chronic pelvic pain, type and amount of prostate cell infiltration and secretion of inflammatory mediators. Our results corroborate and support the notion that mice with different genetic background have different susceptibility to EAP induction, and confirm the high susceptibility of NOD mice to EAP induction.

## ACKNOWLEDGMENTS

This research was supported by grants from Agencia Nacional de Promoción Científica y Tecnológica (ANPCYT) PICT 2008–1639 and 2013–2201, Secretaría de Ciencia y Técnica de la Universidad Nacional de Córdoba (Secyt). MLB and LRS are PhD fellows from CONICET. RDM and VER are members of the Researcher Career of CONICET. We thank Paula Icely, Paula Abadie and Pilar Crespo for excellent technical assistance. We also thank Carolina Florit, Victoria Blanco, Fabricio Navarro and Diego Lutti for animal care.

## REFERENCES

1. Collins MM, Stafford RS, O'Leary MP, Barry MJ. How common is prostatitis? A national survey of physician visits. *J Urol* 1998;159:1224–1228.
2. Habermacher GM, Chason JT, Schaeffer AJ. Prostatitis/chronic pelvic pain syndrome. *Annu Rev Med* 2006;57:195–206.
3. Schaeffer AJ. Clinical practice. Chronic prostatitis and the chronic pelvic pain syndrome. *N Engl J Med* 2006;355:1690–1698.
4. McNaughton Collins M, Pontari MA, O'Leary MP, Calhoun EA, Santanna J, Landis JR, Kusek JW, Litwin MS. Quality of life is impaired in men with chronic prostatitis: The chronic prostatitis collaborative research network. *J Gen Intern Med* 2001;16:656–662.
5. Rivero VE, Motrich RD, Maccioni M, Riera CM. Autoimmune etiology in chronic prostatitis syndrome: An advance in the understanding of this pathology. *Crit Rev Immunol* 2007;27:33–46.
6. Motrich RD, Maccioni M, Molina R, Tissera A, Olmedo J, Riera CM, Rivero VE. Presence of INF gamma-secreting lymphocytes specific to prostate antigens in a group of chronic prostatitis patients. *Clin Immunol* 2005;116:149–157.
7. Motrich RD, Maccioni M, Riera CM, Rivero VE. Autoimmune prostatitis: State of the art. *Scand J Immunol* 2007;66:217–227.
8. Vykhovanets EV, Resnick MI, MacLennan GT, Gupta S. Experimental rodent models of prostatitis: Limitations and potential. *Prostate Cancer Prostatic Dis* 2007;10(1):15–29.
9. Rivero VE, Cailleau C, Depiante-Depauli M, Riera CM, Carnaud C. Non obese diabetic (NOD) mice are genetically susceptible to experimental autoimmune prostatitis (EAP). *J Autoimmun* 1998;11:603–610.
10. Penna G, Amuchastegui S, Cossetti C, Aquilano F, Mariani R, Giarratana N, De Carli E, Fibbi B, Adorini L. Spontaneous and prostatic steroid binding protein peptide-induced autoimmune prostatitis in the nonobese diabetic mouse. *J Immunol* 2007;179:1559–1567.
11. Rivero V, Carnaud C, Riera CM. Prostatein or steroid binding protein (PSBP) induces experimental autoimmune prostatitis (EAP) in NOD mice. *Clin Immunol* 2002;105:176–184.
12. Robinette CL. Sex-hormone-induced inflammation and fibromuscular proliferation in the rat lateral prostate. *Prostate* 1988;12:271–286.
13. Harris MT, Feldberg RS, Lau KM, Lazarus NH, Cochrane DE. Expression of proinflammatory genes during estrogen-induced inflammation of the rat prostate. *Prostate* 2000;44:19–25.
14. Keetch DW, Humphrey P, Ratliff TL. Development of a mouse model for nonbacterial prostatitis. *J Urol* 1994;152:247–250.
15. Motrich RD, van Etten E, Baeke F, Riera CM, Mathieu C, Rivero VE. A crucial role of INFγ in experimental autoimmune prostatitis. *J Urol* 2010;183:1213–1220.
16. Penna G, Amuchastegui S, Cossetti C, Aquilano F, Mariani R, Sanvito F, Doglioni C, Adorini L. Treatment of experimental autoimmune prostatitis in nonobese diabetic mice by the vitamin D receptor agonist elocalcitol. *J Immunol* 2006;177:8504–8511.
17. Breser ML, Motrich RD, Sanchez LR, Mackern-Oberti JP, Rivero VE. Expression of CXCR3 on specific T cells is essential for homing to the prostate gland in an experimental model of chronic prostatitis/chronic pelvic pain syndrome. *J Immunol* 2013;190:3121–3133.
18. Motrich RD, Maccioni M, Ponce AA, Gatti GA, Oberti JP, Rivero VE. Pathogenic consequences in semen quality of an autoimmune response against the prostate gland: From animal models to human disease. *J Immunol* 2006;177:957–967.
19. Motrich RD, Breser ML, Sanchez LR, Godoy GJ, Prinz I, Rivero VE. 2016. IL-17 is not essential for inflammation and chronic pelvic pain development in an experimental model of chronic prostatitis/chronic pelvic pain syndrome. *Pain* 2016;157(3):585–597.
20. Rudick CN, Schaeffer AJ, Thumbikat P. Experimental autoimmune prostatitis induces chronic pelvic pain. *Am J Physiol Regul Integr Comp Physiol* 2008;294:R1268–R1275.
21. Jarrell J. Demonstration of cutaneous allodynia in association with chronic pelvic pain. *J Vis Exp* 2009;(28): pii 1232. DOI: 10.3791/1232
22. Jarrell J, Giamberardino MA, Robert M, Nasr-Esfahani M. Bedside testing for chronic pelvic pain: Discriminating visceral from somatic pain. *Pain Res Treat* 2011;2011:692102.
23. Tsai S, Santamaria P. MHC class II polymorphisms, autoreactive T-Cells, and autoimmunity. *Front Immunol* 2013;4:321.
24. Siggs OM, Makaroff LE, Liston A. The why and how of thymocyte negative selection. *Curr Opin Immunol* 2006;8(2):175–183.
25. Danke NA, Koelle DM, Yee C, Beheray S, Kwok WW. Autoreactive T cells in healthy individuals. *J Immunol* 2004;172(10):5967–5972.
26. Murphy SF, Schaeffer AJ, Thumbikat P. Immune mediators of chronic pelvic pain syndrome. *Nat Rev Urol* 2014;11(5):259–269.
27. Cantor J, Haskins K. Recruitment and activation of macrophages by pathogenic CD4 T cells in type 1 diabetes: Evidence for involvement of CCR8 and CCL1. *J Immunol* 2007;179(9):5760–5767.
28. Ejrnaes M, Videbaek N, Christen U, Cooke A, Michelsen BK, von Herrath M. Different diabetogenic potential of autoaggressive CD8+ clones associated with IFN-gamma-inducible protein 10 (CXC chemokine ligand 10) production but not cytokine expression, cytolytic activity, or homing characteristics. *J Immunol* 2005;174(5):2746–2755.
29. Roman K, Done JD, Schaeffer AJ, Murphy SF, Thumbikat P. Tryptase-PAR2 axis in experimental autoimmune prostatitis, a model for chronic pelvic pain syndrome. *Pain* 2014;155(7):1328–1338.
30. Sayed BA, Christy A, Quirion MR, Brown MA. The master switch: The role of mast cells in autoimmunity and tolerance. *Ann Rev Immunol* 2008;26:705–739.
31. Walker ME, Hatfield JK, Brown MA. New insights into the role of mast cells in autoimmunity: Evidence for a common mechanism of action? *Biochim Biophys Acta* 2012;1822:57–65.
32. Thacker MA, Clark AK, Marchand F, McMahon SB. Pathophysiology of peripheral neuropathic pain: Immune cells and molecules. *Anesth Analg* 2007;105:838–847.
33. Ralainirina N, Brons NH, Ammerlaan W, Hoffmann C, Hentges F, Zimmer J. Mouse natural killer (NK) cells express the nerve growth factor receptor TrkA, which is dynamically regulated. *PLoSOne* 2010;5(12):e15053.
34. Samah B, Porcheray F, Gras G. Neurotrophins modulate monocyte chemotaxis without affecting macrophage function. *Clin Exp Immunol*. 2008;51(3):476–486.
35. Done JD, Rudick CN, Quick ML, Schaeffer AJ, Thumbikat P. Role of mast cells in male chronic pelvic pain. *J Urol* 2012;187:1473–1482.

36. Watanabe T, Inoue M, Sasaki K, Araki M, Uehara S, Monden K, Saika T, Nasu Y, Kumon H, Chancellor MB. Nerve growth factor level in the prostatic fluid of patients with chronic prostatitis/chronic pelvic pain syndrome is correlated with symptom severity and response to treatment. *BJU Int* 2011;108:248–251.
37. Correa SG, Riera CM. Adjuvant effect of liposomes in the autoimmune response to rat male accessory glands. *Immunol Lett* 1991;28:39–46.
38. Rivero VE, Iribarren P, Riera CM. Mast cells in accessory glands of experimentally induced prostatitis in male Wistar rats. *Clin Immunol Immunopathol* 1995;74:236–242.
39. Bromley SK, Mempel TR, Luster AD. Orchestrating the orchestrators: Chemokines in control of T cell traffic. *Nat Immunol* 2008;9(9):970–980.
40. Bono MR, Elgueta R, Sauma D, Pino K, Osorio F, Michea P, Fierro A, Roseblatt M. The essential role of chemokines in the selective regulation of lymphocyte homing. *Cytokine Growth Factor Rev* 2007;18:33–43.
41. Sallusto F, Impellizzeri D, Basso C, Laroni A, Uccelli A, Lanzavecchia A, Engelhardt B. T-cell trafficking in the central nervous system. *Immunol Rev* 2012;248:216–227.
42. Sawant KV, Xu R, Cox R, Hawkins H, Sbrana E, Kolli D, Garofalo RP, Rajarathnam K. Chemokine CXCL1-mediated neutrophil trafficking in the lung: Role of CXCR2 activation. *J Innate Immun* 2015;7(6):647–658.
43. Schnoor M, Alcaide P, Voisin MB, van Buul JD. Crossing the vascular wall: Common and unique mechanisms exploited by different leukocyte subsets during extravasation. *Mediators Inflamm* 2015;2015:946509.
44. Wilson MJ, Woodson M, Wiehr C, Reddy A, Sinha AA. Matrix metalloproteinases in the pathogenesis of estradiol-induced nonbacterial prostatitis in the lateral prostate lobe of the Wistar rat. *Exp Mol Pathol* 2004;77(1):7–17.
45. Busiek DF, Baragi V, Nehring LC, Parks WC, Welgus HG. Matrilysin expression by human mononuclear phagocytes and its regulation by cytokines and hormones. *J Immunol* 1995;154(12):6484–6491.
46. Kang T, Yi J, Guo A, Wang X, Overall CM, Jiang W, Elde R, Borregaard N, Pei D. Subcellular distribution and cytokine- and chemokine-regulated secretion of leukolysin/MT6-MMP/MMP-25 in neutrophils. *J Biol Chem* 2001;276(24):21960–21968.
47. Shapiro SD. Diverse roles of macrophage matrix metalloproteinases in tissue destruction and tumor growth. *Thromb Haemost* 1999;82(2):846–849.
48. Marco M, Fortin C, Fulop T. Membrane-type matrix metalloproteinases: Key mediators of leukocyte function. *J Leukoc Biol* 2013;94(2):237–246.